

Mean field approach to the instanton-induced effects close to the QCD phase transition

M. Velkovsky and E. Shuryak

Department of Physics, State University of New York, Stony Brook, New York 11794

(Received 23 April 1997)

It was suggested earlier that the chiral phase transition is driven by a transition from random instanton–anti-instanton liquid to correlated instanton–anti-instanton molecules. So far this phenomenon was studied by numerical simulations, while we develop an alternative semianalytic approach. For two massless quark flavors, both instantons and “molecules” generate specific four-fermion effective interactions. After those are derived, we determine the temperature dependence of the thermodynamic quantities, the quark condensate, and the fraction of molecules using the standard mean field method. Using the Bethe-Salpeter equation, we calculate the T -dependence of mesonic correlation functions. These results shed new light on the problem of modification of hadrons, and they can be tested directly in lattice simulations. [S0556-2821(97)04515-3]

PACS number(s): 12.38.Lg, 05.70.-a, 11.30.Rd

I. INTRODUCTION

The nature of the chiral restoration phase transition at the critical temperature $T_c \approx 150$ MeV remains one of the main problems in nonperturbative QCD. Not only is it important to understand it from a theoretical point of view, but it is also the motivation for current and future heavy-ion collision experiments. Major efforts are also being made to simulate finite- T QCD on the lattice, and many results have clarified to some extent the phase diagram of QCD-related theories, see reviews [1,2].

At zero temperature the mechanism of spontaneous chiral symmetry breaking and even the very existence of most light hadrons is connected with instantons. The quark condensate is made of the fermionic (quasi)zero modes generated by them. The specific instanton-based picture suggested in [3] was studied both analytically [4,6] and numerically [7–11]. Even the simplest random model (RILM) reproduces well multiple mesonic and baryonic correlation functions, as is known from phenomenology [12] and lattice simulations [13]. Furthermore, the “instanton liquid” itself, with parameters close to those predicted, was “distilled” from lattice configurations [14–16].

It is less clear what happens with instantons at finite temperature T . It has been known for a long time that at *high* T the instanton density is suppressed by Debye-type screening [17,18], and it was first suggested that their disappearance may be the major reason for chiral symmetry restoration (see, e.g., [19]). However recent theoretical analysis at *low* T [20] shows that up to T_c the instanton density can only change a little, and lattice numerical simulations [21] have confirmed that. Therefore, an instanton suppression cannot be an explanation, and a better idea was needed.

Another mechanism suggested in [22] is driven by “pairing” of instantons and antiinstantons into $I\bar{I}$ “molecules.” A two-component (also called “cocktail”) model was used for the description of the low-temperature ($T < T_c$) phase. In it the individual instantons and “molecules” coexist in

ensemble.¹ In the high-temperature phase $T > T_c$ (for $m = 0$) only molecules survive, and therefore the chiral symmetry gets restored. In [11] the cocktail model was studied numerically, by keeping the temperature fixed and changing the “molecule fraction” f . Many mesonic and baryonic correlation functions were calculated: they show very dramatic changes as f goes from small values to 1. Furthermore, a very interesting hint for the survival of some hadrons *above* the phase transition were presented. It was shown that the molecules start to form only close to T_c , and that they are polarized in color space as well as in the Euclidean time direction, as anticipated in [10,22].

This scenario of the phase transition was recently confirmed by numerical simulations of the instanton vacuum at finite temperature in which both boson- and fermion-induced interactions between the pseudoparticles are taken into account [23,25]. In this approach there is no artificial separation between random and “molecular” components, and all correlations follow from the general statistical sum. Still the basic scenario with rapid growth of correlation right below T_c was observed. All basic properties of the chiral restoration phase transition were reproduced, including the transition temperature, its order (second for $N_f = 2$ and first for $N_f > 2$), spectrum of “screening masses,” etc. Furthermore, correlation functions that have been calculated in [25], imply dramatic modifications of hadrons in the low- T phase, close to the transition point.

The objective of the present paper is to study analytically several issues related to these ideas. First of all, we study a single instanton–anti-instanton molecule in much greater detail than ever done before. We found that the configuration discussed previously, with a separation in time equal to half Matsubara time $1/2T$, develops a true maximum of the partition function starting from $T = 0.85T_c$. We also calculated

¹Of course, it is an approximation, modeling a variety of possible states ranging from uncorrelated (random) instantons to strongly correlated ones (molecules).

its contribution using the saddle-point method.

The second step is to deduce the effective Lagrangian, describing interaction between quarks. With T approaching T_c , it changes from the 't Hooft one typical for random liquid to a ‘‘molecule-induced’’ one derived in [23]. Methodically we deviate significantly from the numerical simulations mentioned, which first calculate quark propagation in a *given* background field (a superposition of instantons), averaging over gauge fields *later*. We integrate first over the collective variables of instantons, deriving the *effective interaction* between quarks, and then solve the resulting fermion theory by using the random phase approximation. Basically, here we follow the same well-trod path as used the Bardeen-Cooper-Schrieffer theory of superconductivity or Nambu–Jona-Lasinio model of chiral symmetry breaking.

We decided in this paper to concentrate on the basic case of two massless flavors, although all calculations can (and should) be generalized to a different number of flavors and/or variable quark masses. The case we study is not far from the real world, but it much simpler because of an exact chiral symmetry and only four-fermion-type interactions. Still, the effective interaction is much more complicated than used, e.g., in the NJL approach, it includes two types of nonlocal terms—one from the random instantons and anti-instantons, and the other from the strongly correlated pairs or molecules. The weights of those are T dependent, determined by a maximum of the partition function of the system. It is calculated in a standard Hartree-Fock approximation, reducing the problem to that of free fermions, but with temperature and (which is even more important) momentum-dependent mass.

Finally, in Sec. V we address the issue of hadron modification with T approaching T_c . We have calculated a set of various mesonic correlation functions, using the Bethe-Salpeter equation. As it is well known, because of finite time extension $\tau=1/T$ those do not directly provide masses of the lowest states. However, they still give a very nontrivial information about the interaction between quarks at these conditions. Furthermore, all of these results can be directly tested in lattice calculations, which we hope will be done soon.

Among our results a notable one is a very different behavior of the pion decay constant f_π and the coupling to pseudoscalar current λ_π : f_π vanishes at $T=T_c$, but λ_π does not. We have found an emerging attractive force in the vector channel, which may be relevant to enhancement of the low-mass dilepton production observed in heavy-ion collisions. Finally, we discuss the issue of restoration of the U(1) chiral symmetry.

II. THE $I\bar{I}$ MOLECULES AROUND T_c

This section is relatively independent of the rest of the paper in the sense that it deals with properties of the *single* $I\bar{I}$ molecule. It consists of two steps: the first is a new calculation of the $I\bar{I}$ interaction in the relevant configuration (that is, the quantum mechanics of quarks), while the second deals with the internal dynamics of a molecule, here we integrate

over its collective variables.² In the next sections we will proceed to the statistical ensemble of *multiple* instantons and ‘‘molecules’’ around the critical temperature.

The $I\bar{I}$ interaction and the overlap matrix elements of the fermionic zero modes, both at zero and at finite temperature, were studied in detail in [24]. Unfortunately these studies were not complete in the sense that they did not include our region of interest—the configurations in which the pseudoparticles lie around the opposite ends of a diameter on the Matsubara circle.

The best definition of the *classical* $I\bar{I}$ interaction $S_{\text{int}}=(S-2S_0)$, where S_0 is the single instanton action, is given by the so-called streamline configurations [26]. Unfortunately, at finite temperature, the conformal symmetry that allows to find the streamline is missing. Therefore, one has to use some ansatz for the $I\bar{I}$ configuration which has a natural extension to nonzero T . We are going to use the ratio ansatz [7]

$$A_\mu^a(x) = -\frac{1}{g} \frac{O_I^{ab} \bar{\eta}_{\mu\nu}^b \partial_\nu \Pi_I + O_{\bar{I}}^{ab} \eta_{\mu\nu}^b \partial_\nu \Pi_{\bar{I}}}{\Pi_I + \Pi_{\bar{I}} - 1}, \quad (1)$$

where $\Pi_I = \Pi(x-z_I)$, $\Pi_{\bar{I}} = \Pi(x-z_{\bar{I}})$ and

$$\Pi(\mathbf{r}, t) = 1 + \frac{\pi T \rho^2}{r} \frac{\sinh(2\pi r T)}{\cosh(2\pi r T) - \cos(2\pi t T)}, \quad (2)$$

which is free from the artifacts of the sum ansatz and provides a reasonable repulsive core. The classical bosonic interaction is just obtained from this expression, by numerical calculation of the classical action.

The quark-induced interaction is described in general by fermionic zero-mode overlap matrix element

$$T_{I\bar{I}} = \int dt d^3\mathbf{x} \phi_I^\dagger(x-z_I) \mathcal{D} \phi_{\bar{I}}(x-z_{\bar{I}}). \quad (3)$$

In this case we use the simplest sum ansatz [27], because in this case one can use an ordinary derivative instead of a covariant one. As it was shown in [24], the results in this case differ insignificantly from the ones obtained by the ratio ansatz. Further we shall use $\mathbf{T}_{I\bar{I}}$ to denote the overlap matrix element within one molecule.

The O(3) symmetry of the $I\bar{I}$ configuration along the Matsubara circle allows us to reduce the above integral and the integral for the bosonic part of the action to a two-dimensional one, and we perform the integration numerically. Our results numerically agree with the ones from [24] in the region where their formulas are valid (for Matsubara time separations that are not close to $L/2=1/2T$). The results for $\mathbf{T}_{I\bar{I}}$ are shown in Fig. 1(a), and the combined $e^{-S_{\text{int}}}\mathbf{T}_{I\bar{I}}^4$ in Fig. 1(b) (the dotted line).

The second step is to solve the dynamics of the molecule itself. In another language, one has to account for a multiplicity of different $I\bar{I}$ configurations, or take the integral

²For ordinary molecules, these two steps are analogous to quantum mechanics of electrons (orbitals) and then of nuclear motion.

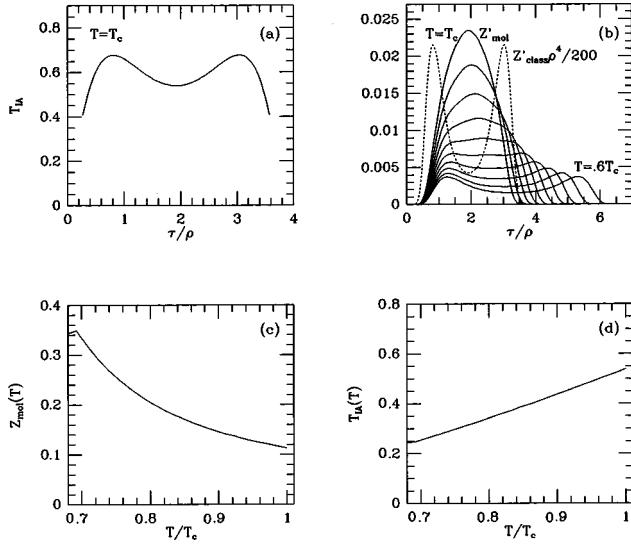


FIG. 1. (a) The time dependence of \mathbf{T}_{II} at T_c , (b) the time dependence of $Z'_{mol}(\tau) = \int d^{10}\Omega T_{II}^4 e^{-S_{int}}$ (the integration over all variables but the Matsubara time), at T_c and at several values of the temperature down to $0.6T_c$, compared to the time dependence of $T_{II}^4 e^{-S_{int}}$ at the saddle point with respect to the above variables and at T_c (the dotted line), (c) the temperature dependence of Z_{mol} , (d) the temperature dependence of \mathbf{T}_{II} .

$$Z_{mol}(T) = \int d^{11}\Omega \mathbf{T}_{II}^{2N_f} e^{-S_{int}} \quad (4)$$

over all collective variables. These are the time separation τ , the three-dimensional spatial separation, and, for SU(3), seven relative orientation angles.³ Most of the 11-dimensional integrals, however, can be done using a saddle-point approximation. Both S_{int} and \mathbf{T}_{II} decay exponentially in the spatial separation directions. The second derivatives of S_{int} over orientation angles are big, because they are multiplied by $8\pi^2/g^2 = S_0 \sim 10 \gg 1$. In contrast to that, the angular dependence of $-2N_f \ln(\mathbf{T}_{II})$ is rather weak, so in angular integrals we treat \mathbf{T}_{II} as a constant. Finally, we find that the saddle-point approximation is not good at all for the integral along the time separation τ .⁴ That is why we perform this last integration explicitly.

In Fig. 1(b), we show the time dependence of $Z'_{mol}(\tau) = \int d^{10}\Omega \mathbf{T}_{II}^4 e^{-S_{int}}$ (the integration over all variables but the Matsubara time), at T_c and at several values of the temperature down to $0.6T_c$, compared to the time dependence of the integrand $\mathbf{T}_{II}^4 e^{-S_{int}}$ at the saddle point with respect to the above variables and at T_c (the dotted line), which has a maximum at about $\tau = L/4$ and a *minimum* at $\tau = L/2$. One can see that around T_c when the multiplicity of

³Note that rotations in the direction of λ_8 does not change the \bar{II} configuration, so that we have only seven orientation parameters. The measure of integration is described in [28].

⁴For example the second derivative of $S_{int} - 2N_f \ln(\mathbf{T}_{II})$ along this direction for a time separation of $L/2$, is negative for temperatures $T < 230$ MeV, although explicit calculations show that this configuration is a maximum for z and not a minimum.

phase space is included, the \bar{II} molecules are distributed around $\tau = 1/2T$, however, at lower temperatures this maximum disappears, so the molecules that we consider play a role only at high enough temperature. The corresponding time dependence of \mathbf{T}_{II} at T_c , which is shown in Fig. 1(a), is rather weak around the maximum of Z' . This allows us to use its central value for all molecules that participate in our ‘‘cocktail model.’’ After the last integral is done, one gets the absolute value of the statistical sum for molecules Z_{mol} . The temperature dependence of Z_{mol} and \mathbf{T}_{II} is shown in Figs. 1(c), 1(d).

How accurate is our saddle-point integration? In the next section we will find that in order to set the phase transition at $T_c = 150$ MeV one needs Z_{mol} about 1.8 larger: it means only a 5–10% error per integration over each of the \bar{II} collective parameters. However, we think the real uncertainty in Z_{mol} is larger, and it is about one order of magnitude [as one can judge from including $-4\ln(\mathbf{T}_{II})$ in the second derivative over the orientation parameters, etc.]. Nevertheless we think its *temperature dependence* is evaluated reliably, and we use it below in our calculation of the thermodynamic properties of the instanton ensemble, the correlation functions, and the pion coupling constants.

III. EFFECTIVE FOUR-FERMION INTERACTION AT FINITE T

Let us first recall how, for one instanton, one derives the well-known 't Hooft effective interaction. The quark propagator includes the zero-mode part

$$S(x, y) = S_{NZM}(x, y) + \frac{\phi_I(x - z_I) \phi_I^\dagger(y - z_I)}{-im}, \quad (5)$$

where $\phi(x)$ is the quark zero mode in the field of an instanton with center at z_I and $S_{NZM}(x, y)$ represent contributions of nonzero modes (following [4] we shall approximate these contributions by the free quark propagator S_0). For N_f light fermions, one should take the Green function with the N_f th power of $S(x, y)$, multiply it by the instanton probability ($P \sim m^{N_f}$). Now powers of m can be canceled, resulting in the $2-N_f$ -fermion interaction which is finite in the chiral limit ($m=0$).

A similar procedure can be repeated for an isolated \bar{II} molecule [23]: only in this case there are two *low-lying* fermionic states. The quark propagator contains the part

$$S_m(x, y) = S_{\text{other modes}}(x, y) + \frac{\phi_{I(m)}(x - (z_m - L/4)) \phi_{I(m)}^\dagger(y - (z_m + L/4))}{\mathbf{T}_{II}} + \frac{\phi_{\bar{I}(m)}(x - (z_m + L/4)) \phi_{\bar{I}(m)}^\dagger(y - (z_m - L/4))}{\mathbf{T}_{II}}, \quad (6)$$

where \mathbf{T}_{II} was defined in Eq. (3).

To get the effective partition function, we generalize the method of ‘‘fermionization,’’ first developed in [5]. The fermion determinant (which appear in the QCD partition function after formal integration over the fermion fields) can be split into the ‘‘zero-mode part’’ and the ‘‘nonzero-mode part.’’ The former can be written as a sum of all closed

diagrams of the N th order in the 't Hooft interaction, for configurations with $N/2$ instantons and $N/2$ antiinstantons. The latter is usually approximated perturbatively.

For the case we are interested in, with some number of strongly correlated $\bar{I}I$ pairs, the zero-mode part of the Dirac matrix has the form

$$\begin{array}{cccc|cccc} 0 & T_{I_1\bar{I}_1} & \cdots & 0 & T_{I_1\bar{I}_{N+1}} & 0 & T_{I_1\bar{I}_{N+2}} & \cdot \\ T_{\bar{I}_1 I_1} & 0 & \cdots & T_{\bar{I}_1 I_{N+1}} & 0 & T_{\bar{I}_1 I_{N+1}} & 0 & \cdot \\ \vdots & \vdots & \ddots & \vdots & \vdots & \vdots & \vdots & \vdots \\ 0 & T_{I_{N+1}\bar{I}_1} & \cdots & 0 & \mathbf{T}_{I_{N+1}\bar{I}_{N+1}} & 0 & T_{I_{N+1}\bar{I}_{N+2}} & \cdot \\ T_{\bar{I}_{N+1} I_1} & 0 & \cdots & \mathbf{T}_{\bar{I}_{N+1} I_{N+1}} & 0 & T_{\bar{I}_{N+1} I_{N+2}} & 0 & \cdot \\ 0 & T_{I_{N+2}\bar{I}_1} & \cdots & 0 & T_{I_{N+2}\bar{I}_{N+1}} & 0 & \mathbf{T}_{I_{N+2}\bar{I}_{N+2}} & \cdot \\ T_{\bar{I}_{N+2} I_1} & 0 & \cdots & T_{\bar{I}_{N+2} I_{N+1}} & 0 & \mathbf{T}_{\bar{I}_{N+2} I_{N+2}} & 0 & \cdot \\ \vdots & \vdots & \vdots & \vdots & \vdots & \vdots & \vdots & \cdot \end{array} \quad (7)$$

Note that some matrix elements (denoted by bold letters) are large: those correspond to quarks exchanged inside the molecules (and were evaluated in the previous section). Our goal is to take them into account, so that in the new effective fermion determinant only small (lightface italic) matrix element remain.

For this goal we reintroduce new fermions, reproducing the zero-mode part of the determinant without intermolecule lines. It is equivalent to closed loops in $(N_+ + N_- + N_m)$ -th order in the fermionic interaction, for configuration with N_+ , N_- , and N_m number of instantons, anti-instantons, and molecules. The interaction due to molecules explicitly includes large $\mathbf{T}_{I\bar{I}}$ matrix elements. Between the interaction points quarks travel with the free propagator:

$$\begin{aligned} T_{I\bar{I}} &= \int d^4x \phi_I^\dagger(x-z_I) \mathcal{D} \phi_{\bar{I}}(x-z_{\bar{I}}) \\ &= \int d^4y d^4x \phi_I^\dagger(y-z_I) i \not{\partial} i S_0 \\ &\quad \times (x-y) i \not{\partial} \phi_{\bar{I}}(x-z_{\bar{I}}) \\ &\rightarrow \int d^4y \phi_I^\dagger(y-z_I) i \not{\partial} \psi_f(y) \\ &\quad \times \int d^4x \psi_f^\dagger(x) i \not{\partial} \phi_{\bar{I}}(x-z_{\bar{I}}), \end{aligned} \quad (8)$$

where we have used the sum ansatz to go from $\not{\partial}$ to \mathcal{D} .

We consider here the $N_f=2$ case only. The one flavor case is not interesting (no restoration of the symmetry) while in the three-flavor case one has a six-fermion interaction, which can only be reduced to a four-fermion one relevant for mesonic channels if some quark masses (e.g., the strange quark mass) are nonzero.

For the $N_f=2$ case in the approximation discussed, the following fermionic path integral gives the effective partition function:

$$\begin{aligned} Z &= \int d\psi d\psi^\dagger \frac{\exp\{\int d^4x \psi^\dagger i \not{\partial} \psi\}}{N_+! N_-! N_m!} \prod_{I=1}^{N_+} c_\rho \theta_+ \\ &\quad \times \prod_{\bar{I}=1}^{N_-} c_\rho \theta_- \prod_{m=1}^{N_m} c_\rho^2 \frac{c}{T_{I\bar{I}}} \theta_m. \end{aligned} \quad (9)$$

One can see, that it indeed generates the propagators (5), (6). Here

$$\begin{aligned} \theta_+ &= \int dz_I d\Omega_I \prod_{f=1}^2 \left(\int d^4x \psi_f^\dagger(x) i \not{\partial} \phi_f(x-z_I) \right. \\ &\quad \left. \times \int d^4y \phi_f^\dagger(y-z_I) i \not{\partial} \psi_f(y) \right), \end{aligned} \quad (10)$$

$$\begin{aligned} \theta_- &= \int dz_{\bar{I}} d\Omega_{\bar{I}} \prod_{f=1}^2 \left(\int d^4x \psi_f^\dagger(x) i \not{\partial} \phi_{\bar{I}}(x-z_{\bar{I}}) \right. \\ &\quad \left. \times \int d^4y \phi_{\bar{I}}^\dagger(y-z_{\bar{I}}) i \not{\partial} \psi_f(y) \right), \end{aligned} \quad (11)$$

$$\begin{aligned} \theta_m &= \int dz_m d\Omega_m \mathbf{T}_{I\bar{I}}^2 \left\{ \mathbf{T}_{I\bar{I}}^2 + \prod_{f=1}^2 \left[\int d^4x \psi_f^\dagger(x) i \not{\partial} \phi_{I(m)} \right. \right. \\ &\quad \left. \left. \times \left(x-z_m + \frac{L}{4} \right) \int d^4y \phi_{\bar{I}(m)}^\dagger \left(y-z_m - \frac{L}{4} \right) i \not{\partial} \psi_f(y) \right. \right. \\ &\quad \left. \left. + \int d^4x \psi_f^\dagger(x) i \not{\partial} \phi_{\bar{I}(m)} \left(x-z_m - \frac{L}{4} \right) \right. \right. \end{aligned}$$

$$\begin{aligned}
& \times \int d^4y \phi_{I(m)}^\dagger \left(y - z_m + \frac{L}{4} \right) i \not{\partial} \psi_f(y) \Big] \\
& + \sum_{f=1}^2 \left[\int d^4x \psi_f^\dagger(x) i \not{\partial} \phi_{I(m)} \left(x - z_m + \frac{L}{4} \right) \right. \\
& \times \int d^4y \phi_{I(m)}^\dagger \left(y - z_m + \frac{L}{4} \right) i \not{\partial} \psi_f(y) \\
& \times \int d^4x' \psi_f^\dagger(x') i \not{\partial} \phi_{\bar{I}(m)} \left(x' - z_m - \frac{L}{4} \right) \\
& \left. \times \int d^4y' \phi_{\bar{I}(m)}^\dagger \left(y' - z_m - \frac{L}{4} \right) i \not{\partial} \psi_f(y') \right] \Big\}. \quad (12)
\end{aligned}$$

The expression (12) can be obtained from Eq. (7) by keeping only the terms containing the large matrix elements $\mathbf{T}_{I\bar{I}}^4$ and $\mathbf{T}_{I\bar{I}}^2$ and then applying Eq. (8) as we did for Eqs. (10) and (11). The odd terms in $\mathbf{T}_{I\bar{I}}$ disappear, because of the integration over z_m . Here z_m and Ω_m are the collective coordinates of an $I\bar{I}$ molecule (the coordinates of its center of mass and its global orientation angles), $c = Z_{\text{mol}}/\mathbf{T}_{I\bar{I}}^2$ and c_ρ are the single instanton partition functions (containing all nonzero mode contributions) [30] integrated over the instanton radius ρ . The convergence of the latter is due to the nonperturbative $g(\rho)$, which tends to a constant for large ρ [15,29].

Now, applying the inverse Laplace transformation, we get the partition function

$$\begin{aligned}
Z = \text{const} \int d\beta_+ d\beta_- d\beta_m \exp \Big\{ & -(N_+ + 1) \ln(\beta_+/c_\rho) \\
& - (N_- + 1) \ln(\beta_-/c_\rho) - (N_m + 1) \ln[\beta_m/(c_\rho^2 c)] \\
& + \int d^4x \left(\psi^\dagger i \not{\partial} \psi + \beta_+ \theta_+ + \beta_- \theta_- + \beta_m \frac{\theta_m}{T_{I\bar{I}}^2} \right) \Big\}. \quad (13)
\end{aligned}$$

To evaluate the effective interaction θ_i terms we go to momentum space and do the integrations over the center coordinates of the instantons, anti-instantons, and molecules. Some useful formulas for thus obtained ‘‘density matrices’’ in the zero-temperature case are given by Dyakonov and Petrov in [4], and they are easily generalized to finite temperature. The Fourier transforms of the fermion zero modes at finite temperature are [31]

$$\alpha(\mathbf{k}, \omega_n) = (\mathbf{k}^2 + \omega_n^2)(A^2 + B^2), \quad (14)$$

$$\begin{aligned}
A = \frac{1}{2\pi\rho} \int_0^\infty 4\pi r^2 dr \int_0^{1/T} dt \left(\frac{\cos(kr)}{kr} - \frac{\sin(kr)}{k^2 r^2} \right) \\
\times \cos(\omega_n t) \Pi^{1/2} \partial_r \left(\frac{(\Pi - 1)}{\Pi} \frac{\cos \pi t T}{\cosh \pi r T} \right), \quad (15)
\end{aligned}$$

$$\begin{aligned}
B = \frac{1}{2\pi\rho} \int_0^\infty 4\pi r^2 dr \int_0^{1/T} dt \frac{\sin(kr)}{kr} \\
\times \sin(\omega_n t) \Pi^{1/2} \partial_r \left(\frac{(\Pi - 1)}{\Pi} \frac{\cos \pi t T}{\cosh \pi r T} \right), \quad (16)
\end{aligned}$$

where Π is the potential (2) that also appears in the finite temperature zero modes ϕ^R in coordinate space [32]:

$$\phi^R = \frac{1}{2\pi\rho} \Pi^{1/2} \not{\partial} \left(\frac{(\Pi - 1)}{\Pi} \frac{\cos \pi t T}{\cosh \pi r T} \right) \epsilon^R, \quad (17)$$

and ϵ^R is the standard constant spinor coupling spinor and Dirac indexes.

The next step is to integrate over the orientation angles of the instantons, anti-instantons, and molecules.⁵ After the (four-fermion nonlocal) interaction is obtained, for convenience, one may perform a Fierz transformation, and add the cross-terms to the interaction. (This is called a Fierz symmetric form of the interaction. Of course, when one writes the T matrix element in a Schwinger-Dyson-type of equation, one should not add again the cross channel.) The result has a color singlet and a color octet term (containing the color matrices $t^i \otimes t^j$), which is given in [23]. These terms do not enter the mean field equations (where only scalars with respect to the flavor, color, and space-time appear), nor do they appear in the Bethe-Salpeter equations for the mesons, because they are color singlets. (However, these color octet terms will appear in the Schwinger-Dyson-type equations for diquarks that are important when we consider baryon correlation functions. In our paper we do not consider those.)

Combining all fermion terms together, one obtains the following nonlocal Fierz symmetric four-fermion interaction:⁶

$$\begin{aligned}
S_{4f} = \int \prod_{i=1}^4 \frac{d^4 k_i}{(2\pi)^4} (2\pi)^4 \delta^4(k_1 - k_2 + k_3 - k_4) \\
\times \sqrt{\alpha(k_1)\alpha(k_2)} \sqrt{\alpha(k_3)\alpha(k_4)} \\
\times \left\{ (\beta_+ + \beta_-) \frac{1}{16N_c^2} [(\psi^\dagger \tau_a^- \psi)^2 - (\psi^\dagger \tau_a^- i \gamma_5 \psi)^2] \right. \\
+ \text{octet terms} \Big] - \beta_m \left[\frac{1}{4N_c^2} [(\psi^\dagger \tau_a \psi)^2 + (\psi^\dagger \tau_a i \gamma_5 \psi)^2] \right. \\
- \frac{1}{4N_c^2} [(\psi^\dagger \tau_a \gamma_0 \psi)^2 + (\psi^\dagger \tau_a \gamma_0 \gamma_5 \psi)^2] \\
\left. \left. + \frac{1}{N_c^2} (\psi^\dagger \gamma_0 \gamma_5 \psi)^2 + \text{octet terms} \right] \right\}, \quad (18)
\end{aligned}$$

where $\tau_a^- = (i, \tau)$, while $\tau_a = (1, \tau)$. The last square brackets represent the ‘‘molecular interaction’’ derived in [23]. There

⁵Let us again remind the reader that for the molecules we assume complete polarization both in coordinate and color space.

⁶All expressions throughout the text should be understood as given at finite temperature. In particular, $\int d^4k/(2\pi)^4$ means $T \sum_{n=-\infty}^{\infty} \int d^3\mathbf{k}/(2\pi)^3$, etc.

are no two-fermion terms, because the integral over the orientation of the molecule in color space is zero.

One can view this Lagrangian as a variant of the effective Nambu–Jona-Lasinio model. Note, however, that it is rather different from what is usually used [33,34]: our coupling constants depend on temperature, in a way to be determined in the next section. Also, the interaction is not nonrenormalizable because a natural cutoff is given by the nonlocality of the vertices: multiloop diagrams can (and must) be treated.

IV. THE MEAN FIELD APPROXIMATION AND THERMODYNAMICS

The effective coupling of the interaction described above depends on the number of uncorrelated and correlated instantons: and in order to find those one should ideally be able to calculate the partition function and minimize the free energy. We will indeed do it now, but under many simplifying assumptions. Most of them are just technical, and can be removed later, if needed. They can be made partly because we are primarily interested only in a comparatively narrow interval of temperature T , slightly below T_c , in which significant structural changes (the phase transition) take place.

We fix the total pseudoparticle density to be a constant for T up to $T_c = 150$ MeV, with only composition f changing. We take $n_{\text{tot}} = n_{\text{inst}} + n_{\text{anti-inst}} = 1 \text{ fm}^{-4}$ specifically, lacking a more accurate number. (None of the results change qualitatively if, say, it is modified by a factor of 2.)

Lattice data in [21] indicate, that the instanton radius does not change much with T until well above the phase transition. So we also fix it at $\rho = 0.34$ fm. (However, we are going to express all dimensional quantities in units of ρ and its powers anyway.)

In Sec. II we have shown that the dominant configuration for the $I\bar{I}$ molecules is the one in which the distance between their centers in the Euclidean time direction is equal to ‘half-box’ $R = L/2 \equiv 1/2T$, the spatial distance is 0, and they have the most attractive relative orientation in color space. Although the molecule distribution has some span around $L/2$ in the time direction, $\mathbf{T}_{I\bar{I}}$ changes little, which allows us to use an average value for all molecules.

T_c and S_0 are related by the requirement that all unpaired instantons disappear at T_c . This condition can be satisfied only in a window around $T_c = 150$ MeV. We use the following values: $T_c = 150$ MeV, $S_0 = 9.5$. However, there is a big uncertainty in this relation, due to the uncertainty of the calculated value of the molecule activity Z_{mol} .

We have ignored all bosonic interactions between random instantons and among $I\bar{I}$ molecules.

To calculate the thermodynamic properties of the system, we first bosonize the fermionic action, making Hubbard–Stratonovitch transformation

$$\begin{aligned} & \sqrt{\prod \alpha(k_i) (\psi^\dagger \psi)^2} \\ & \rightarrow 2 \sqrt{\alpha(k_1) \alpha(k_2)} \psi^\dagger(k_1) \psi(k_2) V_4 (2\pi)^4 \delta^4(k_3 - k_4) Q \\ & - V_4^2 (2\pi)^8 \delta^4(k_1 - k_2) \delta^4(k_3 - k_4) Q^2. \end{aligned} \quad (19)$$

Then we consider the bosonic field Q as a constant, to be determined from the grand canonical potential minimization. As there is no net topological charge, $\beta_+ = \beta_- = \beta$. We also define $f = 2N_m/N_{\text{tot}}$, $N_+ = N_- = [(1-f)/2] n_{\text{tot}} V_4$, $N_m = (f/2) n_{\text{tot}} V_4$. After integration over the fermion degrees of freedom we have the following grand canonical potential:⁷

$$\begin{aligned} \frac{\Delta\Omega}{V_4} = & -T_{I\bar{I}} \beta_m + (-f) n_{\text{tot}} \ln\left(\frac{\beta}{c\rho}\right) + \frac{f}{2} n_{\text{tot}} \ln\left(\frac{\beta_m}{c\rho^2 c}\right) \\ & + \frac{Q^2}{8N_c^2} (\beta + 2\beta_m) - 4N_c \int \frac{d^4k}{(2\pi)^4} \ln[k^2 + M^2(k)], \end{aligned} \quad (20)$$

where one can identify the chemical potentials for the ‘liquid’ component $\ln(\beta/c\rho)$ and for the ‘molecular’ one $\ln(\beta_m/c\rho^2 c)$. The last term corresponding to a gas⁸ of massive quarks with the (instanton-induced) momentum-dependent mass

$$M(k) = \frac{\alpha(k)Q(\beta + 2\beta_m)}{4N_c^2}. \quad (21)$$

We shall determine this mass from a self-consistency condition, represented graphically in Fig. 2(a), where the vertex K is a sum of the instanton and the molecular interactions [Fig. 2(b)].

Our next step is minimization of $\Delta\Omega$ with respect to f, β_m, β, Q . There are four equations:

$$\beta_m - c\beta^2 = 0, \quad (22)$$

$$T_{I\bar{I}}^2 - \frac{fn_{\text{tot}}}{2\beta_m} + 8N_c \int \frac{d^4k}{(2\pi)^4} \frac{2M(k)}{k^2 + M^2(k)} \frac{Q\alpha(k)}{4N_c^2} - \frac{Q^2}{4N_c^2} = 0, \quad (23)$$

$$\begin{aligned} -\frac{(1-f)n_{\text{tot}}}{\beta} + 4N_c \int \frac{d^4k}{(2\pi)^4} \frac{2M(k)}{k^2 + M^2(k)} \frac{Q\alpha(k)}{4N_c^2} - \frac{Q^2}{8N_c^2} \\ = 0, \end{aligned} \quad (24)$$

$$4N_c \int \frac{d^4k}{(2\pi)^4} \frac{2M(k)}{k^2 + M^2(k)} \frac{\alpha(k)}{4N_c^2} - \frac{2Q}{8N_c^2} = 0. \quad (25)$$

⁷Note that, our grand canonical potential is not complete in the following sense. The gauge fields are assumed to be only a superposition of instantons, while all excitations of the gluonic degrees of freedom are excluded. In principle, there should be a gluonic term (similar to the last quark term in the action above), which eventually (at high T) will lead to the perturbative gluonic part of the thermal energy. We do not include it because (i) glueballs are much heavier than mesons and constituent quarks, and are not excited at $T \sim T_c = 150$ MeV and (ii) we mainly use the grand canonical potential in order to determine parameters such as f and the quark-related quantities Q, β, β_m . The missing term describing gluonic excitations can hardly affect them.

⁸We remind the reader that the instanton vacuum has no confinement, so free quarks just change their effective mass in the transition.

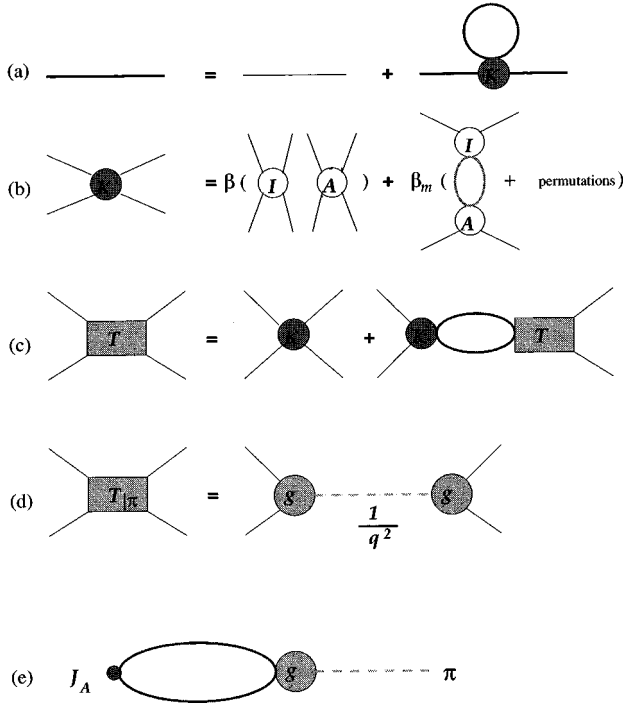


FIG. 2. (a) The Hartree-Fock (self-consistency) equation for the quark propagator. (b) The four-fermion interaction as a sum of the 't Hooft vertex and the molecular vertex. (c) The Bethe-Salpeter equation for the T matrix in the mesonic channels. (d) The pion T matrix near the massless pion pole. (e) The diagram for the pion coupling to the axial current.

One can notice, that the first equation is the condition for chemical equilibrium between the random and molecular components.

As we mentioned in the Introduction, we have chosen not to vary the total density of pseudoparticles, because there are strong theoretical indications that it is not suppressed up to T_c , but we have taken it from the lattice data, which also suggests, that in pure gauge theory it does not change up to temperatures of the order of the deconfinement transition $T \sim 260$ MeV, much higher than those we work with.

Of course, one should in principle perform variation with respect to this quantity, and the additional equation is $\beta = c_\rho$. However this only adds an additional equation to those we solve. Attempts to determine c_ρ have to deal with at least two unsolved problems: (i) the evaluation of the integrated single instanton partition function and (ii) its T dependence at temperatures below T_c , where the Pisarski-Yaffe factor does not exist. The formal expression given by 't Hooft contains a divergent integral over the instanton radius. The interaction effects in the instanton liquid may make the integral convergent, provided there is repulsion. If we use the lattice information for the total density, we can consider $\beta = c_\rho$ as an equation which determines c_ρ as a function of the temperature.

The four equations can be reduced to one "gap" equation, that has to be solved numerically:

$$\frac{2}{N_c} \int \frac{d^4k}{(2\pi)^4} \frac{\beta(1+2c\beta)\alpha^2(k)}{k^2 + \beta(1+2c\beta)^2(1-f)n_{\text{tot}}\alpha^2(k)/(2N_c^2)} = 1, \quad (26)$$

with

$$\beta = \left[-(1-f)n_{\text{tot}} + \sqrt{(1-f)^2 n_{\text{tot}}^2 + f/(2c)n_{\text{tot}} \mathbf{T}_{II}^2} \right] \frac{1}{\mathbf{T}_{II}^2}. \quad (27)$$

At T_c , all unpaired instantons disappear ($f \rightarrow 1$) and the chiral symmetry is restored. The condition $f=1$ is satisfied on a line in the T, S_0 plane. We have chosen $T_c = 150$ MeV $= 0.26/\rho$ and $S_0 = 9.5$. Of course, when $f=1$ or $f=0$, the saddle-point approximation for the β integrals is no longer valid, so our model is restricted in the region $0 < f < 1$, where the saddle-point method is justified in the thermodynamic limit $V_4 \rightarrow \infty$. We see that when $f \rightarrow 1$, $\beta_m = n_{\text{tot}}/(2\mathbf{T}_{II}^2)$, $\beta = \sqrt{n_{\text{tot}}/(2c\mathbf{T}_{II}^2)}$ does not tend to 0, so that the $U_A(1)$ symmetry remains broken when $T \rightarrow T_c$. This can also be seen in our discussion of the correlation functions in Sec. IV. Recall that in the Nambu–Jona-Lasinio model, the coupling constant tends at T_c to the nonzero critical coupling (at which the chiral condensate vanishes and the chiral symmetry is restored). So when the density of the random instanton component goes to zero, the interaction does not disappear. Indeed, as we know from 't Hooft, even when there are no instantons in the vacuum, every external quark current induces them, so we always have some residual 't Hooft interaction.

The opposite limit $f \rightarrow 0$ should not be considered in our model, because as we go down from T_c , the approximations that we have made for the instanton ensemble, namely, that we have uncorrelated instanton liquid and polarized molecules oriented in the time direction, become worse. However, it is worth noticing that although the numerator in Eq. (27) goes to 0, when $f \rightarrow 0$, the denominator also decreases, because the molecules tend to expand and "melt" into the liquid, so β even increases, when we decrease the temperature.

We have not answered the question about the β value above T_c . We can calculate the residual 't Hooft interaction at high temperature, where the integral over the instanton radius is well convergent due to thermal effects, but we cannot extrapolate it towards T_c . Moreover, nothing prevents β from having a discontinuity at T_c , because at T_c ΔF and its first derivatives do not depend on β . So we can conclude that the residual $U_A(1)$ -violating 't Hooft interaction immediately above T_c remains unknown.

Our results are presented in Fig. 3, where the molecule fraction f , the effective quark mass $M(\mathbf{0}, \pi T)$, the quark condensate $\langle \bar{\psi}\psi \rangle$, and the energy density ϵ are presented. Note, that the local $\langle \bar{\psi}\psi \rangle$ has one power of the form factor α less under the momentum integral, compared to the nonlocal mean field Q . $\langle \bar{\psi}\psi \rangle$ is normalized to the phenomenological value of the quark condensate at $T=0$. We see that in about 20 MeV the fraction of the molecules drops to about half, the quark condensate almost reaches its phenomenological value at $T=0$, but the constituent quark mass, which is defined as the value of the momentum-dependent mass from the gap equation at zero spatial momentum and Matsubara frequency πT , is still low—about 1/3 of its phenomenological value at $T=0$. [The reader should be warned that one can hardly compare the mass value obtained in the present calculation

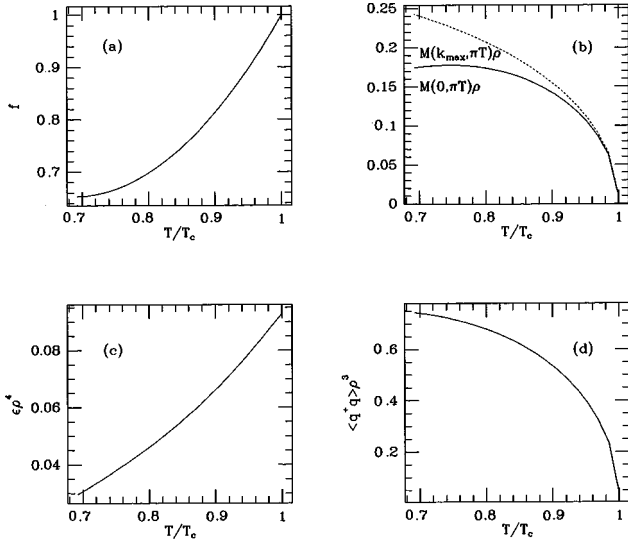


FIG. 3. (a) The molecule fraction f , (b) the effective quark mass $M(\mathbf{0}, \pi T)$ (solid line) and $M(\mathbf{k}_{\max}, \pi T)$ (dotted line), (c) the energy density ϵ , and (d) the quark condensate $\langle \bar{\psi}\psi \rangle$, normalized to the phenomenological value at zero temperature as a function of the temperature. All dimensional quantities are in units of the inverse instanton radius $1/\rho = 580$ MeV.

with the usual constituent quark mass $M(\vec{k}=0, \omega=0) \sim 350$ MeV because the minimal energy possible $\omega \approx \pi T_c$ is rather large.] In addition, the finite temperature form factors have a maximum at spatial momentum $\mathbf{k}_{\max} \neq 0$, so we show with a dotted line the temperature dependence of the mass defined at $k = (\mathbf{k}_{\max}, \pi T)$.

This behavior of the thermodynamic quantities looks similar to the one obtained in [31] or in the NJL models [34], and both are governed by similar gap equations for the constituent quark mass or the quark condensate. However, the physics of the transition in our case is quite different. In [34] the transition is governed by the suppression of the quark condensate by thermal excitations of quarks. In [31] there is an additional thermal suppression of the instanton density, which results in an additional suppression of the effective coupling constant. In our case, the main effect is the reorganization of the instanton vacuum: it leads to reorganization of the Lagrangian by itself. This can be seen by the fact that the mean field Q (a *nonlocal* analogue of the quark condensate), is proportional to the square root of the density of the random component $1-f$. Our mechanism makes the transition region narrower and the transition temperature T_c lower.

In Fig. 4(a) we show the pressure $p = -\Delta F$ (solid line), together with its different components: pressure of free massless fermions $4N_c \int [d^4k/(2\pi)^4] \ln(k^2)$ (open triangles), the deviation from it, due to the effective mass $4N_c \int [d^4k/(2\pi)^4] \ln\{[k^2 + M^2(k)/k^2]\}$ (open squares), the contribution from the condensate $-Q^2/8N_c^2(\beta + 2\beta_m)$ (stars), the contributions from the molecules $T_{17}^2 \beta_m - (f/2)n_{\text{tot}} \ln(\beta_m/c_\rho^2 c)$ (black squares), and the instanton liquid $-(1-f)n_{\text{tot}} \ln(\beta/c_\rho)$ (black triangles). For comparison, we also show that the pressure of a pionic gas $p = 0.987T^4$ (dotted line) is significantly smaller than any of the components under consideration, and thus unimportant.

In Fig. 4(b) the energy density ϵ below the phase transi-

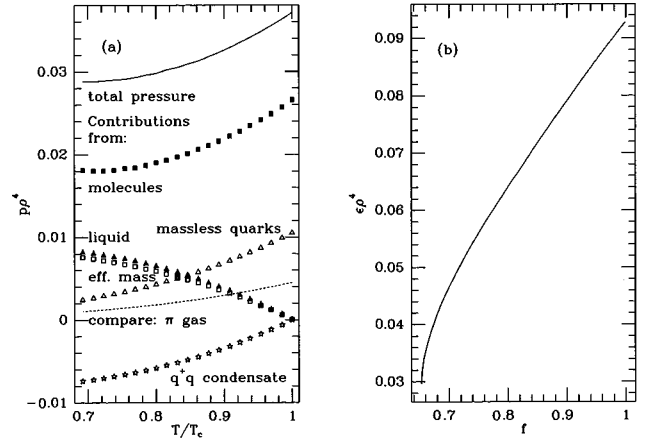


FIG. 4. (a) The pressure $p = -\Delta F$, and its components, as a function of the temperature. The pressure is shown by a solid line and the different contributions to it are as follows: pressure of free massless fermions $4N_c \int [d^4k/(2\pi)^4] \ln(k^2)$ (open triangles), the deviation from it, due to the effective mass $4N_c \int [d^4k/(2\pi)^4] \ln\{[k^2 + M^2(k)/k^2]\}$ (open squares), the contribution from the condensate $-Q^2/8N_c^2(\beta + 2\beta_m)$ (stars), the contributions from the molecules $T_{17}^2 \beta_m - (f/2)n_{\text{tot}} \ln(\beta_m/c_\rho^2 c)$ (black squares), and the instanton liquid $-(1-f)n_{\text{tot}} \ln(\beta/c_\rho)$ (black triangles). For comparison, the pressure of a pion gas is shown by a dotted line. (b) The dependence of the energy density ϵ on the molecule fraction f .

tion point is shown to be actually directly proportional to the molecule fraction f . This correlates well with the observation made in [23], that (unlike the individual instantons) the molecules have a net positive energy, even in the classical approximation.

V. MESONIC CORRELATION FUNCTIONS

Our last step is investigation of the effect of the four-fermion effective interaction on mesonic spectra at $T \approx T_c$. Using the Bethe-Salpeter equation one may calculate mesonic correlation functions, similar to what was done in [33,34]. Our major advantage is that we naturally have non-local vertices, which provide an ultraviolet cutoff. We start with the two-body interaction kernel K , which is given by the four-fermion terms in the effective Lagrangian. Then we have the BS equation for the quark-antiquark T matrix [Fig. 2(c)]:

$$\mathcal{T}(q) = \mathcal{K} + i \text{Tr} \int \frac{d^4P}{(2\pi)^4} \alpha \left(p + \frac{q}{2} \right) \alpha \left(p - \frac{q}{2} \right) \times \left[\mathcal{K} S_F \left(p + \frac{q}{2} \right) \mathcal{T}(q) S_F \left(p - \frac{q}{2} \right) \right]. \quad (28)$$

The trace is taken over the Dirac, flavor, and color matrices. For the colorless meson channels we need only the color singlet terms in the Lagrangian. Then using the symmetries of the Matsubara space-time, we can decompose T and K into covariant structures.

$$\langle \bar{q}_4 q_3 | \mathcal{K} | \bar{q}_2 q_1 \rangle = \sum_{i,\alpha} K_\alpha^i \left[\Gamma_\alpha \frac{\tau^i}{2} \right]_{34} \left[\Gamma_\alpha \frac{\tau^i}{2} \right]_{12}, \quad (29)$$

where $\Gamma\alpha$ denotes Dirac tensors.

Because at $T \neq 0$ there is less symmetry than at zero temperature, we have more structures. However, our particular action (18) contains only scalar and pseudoscalar terms and the time oriented vector and axial terms produced by γ_0 and $\gamma_0\gamma_5$; therefore, only the following coefficients are non-zero:

$$\begin{aligned} K_S^i &= \frac{-1}{4N_c^2} \left[2\beta_m + 2 \left(\delta_{i0} - \frac{1}{2} \right) \beta \right], \\ K_P^i &= \frac{1}{4N_c^2} \left[-2\beta_m + 2 \left(\delta_{i0} - \frac{1}{2} \right) \beta \right], \\ K_V^i &= \frac{1}{2N_c^2} \beta_m, \\ K_A^i &= \frac{1}{2N_c^2} (1 - 4\delta_{i0})\beta_m. \end{aligned} \quad (30)$$

If we define the loop integral:

$$\begin{aligned} J_{\alpha\beta}^{ij}(q) &= iN_c \text{tr} \int \frac{d^4p}{(2\pi)^4} \alpha \left(p + \frac{q}{2} \right) \alpha \left(p - \frac{q}{2} \right) \\ &\times \left[\Gamma_\alpha \frac{\tau^i}{2} S_F \left(p + \frac{q}{2} \right) \Gamma_\beta \frac{\tau^j}{2} S_F \left(p - \frac{q}{2} \right) \right], \end{aligned} \quad (31)$$

then the solution of the Bethe-Sapeter (BS) equation (in matrix notation) is

$$T = [1 - JT]^{-1} K. \quad (32)$$

To get the mesonic correlation function for the corresponding channel, we have to multiply T from the left and the right with two loop integrals J (those have only two form factors $\sqrt{\alpha}$, instead of four, because the correlation function is defined for pointlike currents). For all channels, we have separated equations except for the pseudoscalar and axial vector channels which mix both for isospin 1 (π) and 0 (η). In Fig. 5 we show the Fourier transforms of the correlation functions for Euclidean time separation of the currents, normalized to the free correlation function at finite temperature. We show them in six steps with $\Delta T \approx 9$ MeV, starting from $T = 150$ MeV and ending with $T \approx 105$ MeV.

The most striking feature is the strong attraction in the pion channel, which remains robust and does not disappear at T_c . This is due mainly to the residual 't Hooft interaction (induced by the propagating quarks) and in a lesser extent to the attractive character of the molecular interaction in this channel (triangles). This feature is in agreement with the lattice simulations around T_c [35], which also show a strong pion signal beyond T_c . Furthermore, at T_c our pion signal is

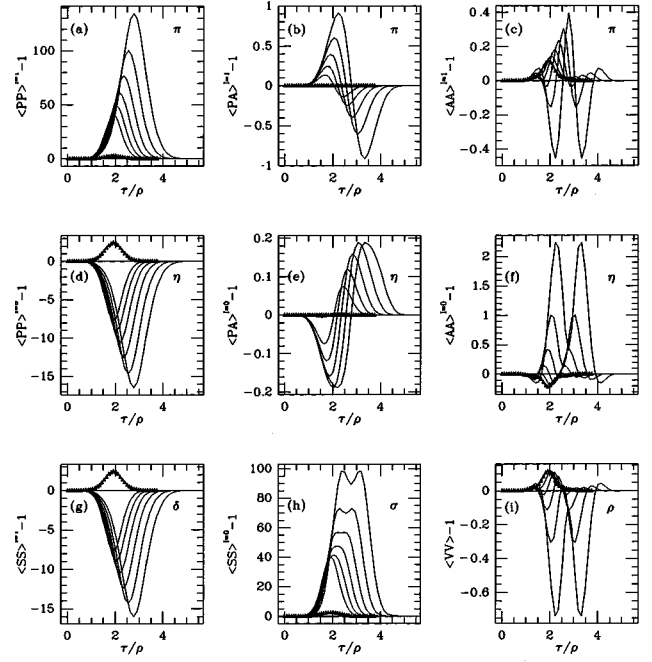


FIG. 5. Mesonic correlation functions for Euclidean time separation of the currents, normalized to the free correlation function at finite temperature. At $\tau=0$ and $\tau=1/T$ they are 1, but we have subtracted 1 for convenience. τ is in units of ρ . These are the isospin 1 pseudoscalar-pseudoscalar (a), pseudoscalar-axial (b), and axial-axial (c) correlators; the isospin 0 pseudoscalar-pseudoscalar (d), pseudoscalar-axial (e), and axial-axial (f) correlators; the scalar-scalar correlators for isospin 1 (g) and 0 (h); and the vector-vector correlators, which are the same for isospin 1 and 0 (i). There are six different temperatures, starting at $T \approx 150$ MeV and ending with $T \approx 105$ MeV. For comparison, the correlation functions of a purely “molecular” vacuum at T_c are plotted with triangles.

similar to the one from the numerical simulations of the interacting instanton liquid [11], although stronger.⁹

The results are in agreement with all chiral theorems, and they clearly show restoration of the chiral symmetry at T_c . In particular, at $T=T_c$ the π pseudoscalar correlation function $\langle PP^1 \rangle$ coincides with the σ scalar correlation function $\langle SS^0 \rangle$. Another feature in agreement with the chiral symmetry is that the pion is decoupled from the axial current ($f_\pi \rightarrow 0$) at $T \rightarrow T_c$, but remains coupled to the pseudoscalar one ($\lambda_\pi \neq 0$) even in the pure molecular vacuum ($f=1$).

An open theoretical issue debated in the literature is *how strongly* the $U_A(1)$ chiral symmetry is violated at $T \sim T_c$, see, e.g., [29,36–38]. We remind the reader that this symmetry is strongly broken by random liquid at low T , but it is respected by the new term in the Lagrangian due to “molecules” which we derived above. Although molecules are prevailing above T_c , the 't Hooft interaction, nevertheless, does not disappear completely at any T . One way to explain it is to say that external currents can always induce additional instantons, absent in vacuum.

The way to measure $U_A(1)$ -violating effects is to calcu-

⁹The differences might be due to the fact that we are considering the chiral limit, while in [11] the quarks have a nonzero mass, which leads to the smearing of all signals.

late the correlation function for η (the isoscalar pseudoscalar) or the isovector scalar, to be referred to as δ , and compare their properties with the pion or σ ones. These two channels are $U_A(1)$ partners of σ and π , and if this symmetry gets (approximately) restored,¹⁰ those should converge.

As shown in [9], in the random instanton vacuum the correlation functions in the η , δ channels, display so strong a repulsive interaction that they become negative.¹¹ Our results show that although the η , δ correlators *increase* when T approaches the phase transition point, the $U(1)$ restoration still does not happen in our model. For comparison, we have

$$T_\pi|_{q_0=0, \mathbf{q}\rightarrow 0} = \frac{[g_P(i\gamma_5\tau_3) + g_A^0(-i\gamma_0\gamma_5\tau_3)] \otimes [g_P(i\gamma_5\tau_3) + g_A^0(i\gamma_0\gamma_5\tau_3)]}{q_0^2 + \mathbf{q}^2}. \quad (33)$$

Comparing with (32), we get:

$$g_P = \sqrt{\left. \frac{K_P^3(1 - K_A^3 J_{A^0 A^0}^{33})}{dD_\pi/dq^2} \right|_{q_0=0, \mathbf{q}\rightarrow 0}}, \quad (34)$$

$$g_A = g_P \left. \frac{(K_A^3 J_{PA^0}^{33})}{(1 - K_A^3 J_{A^0 A^0}^{33})} \right|_{q_0=0, \mathbf{q}\rightarrow 0}, \quad (35)$$

where $D_\pi = \det(1 - K_\pi J_\pi) = (1 - K_P^3 J_{PP}^{33})(1 - K_A^3 J_{AA}^{33}) - K_P^3 K_A^3 (J_{PA}^{33})^2$. Using the definitions

$$if_\pi q^\mu \delta_{ij} = \left\langle 0 \left| \bar{\psi}(0) \gamma^\mu \gamma_5 \frac{\tau^i}{2} \psi(0) \right| \pi_j(q) \right\rangle, \quad (36)$$

$$\lambda_\pi \delta_{ij} = \left\langle 0 \left| \bar{\psi}(0) i \gamma_5 \frac{\tau^i}{2} \psi(0) \right| \pi_j(q) \right\rangle, \quad (37)$$

and calculating a simple loop diagram [Fig. 2(d)], we get

$$\lambda_\pi = \tilde{T}_{PP}^3 g_P, \quad (38)$$

$$f_\pi^0 = (\tilde{T}_{PA^0}^3 / q^0 g_P + \tilde{T}_{A^0 A^0}^3 g_A / q^0)|_{q_0=0, \mathbf{q}\rightarrow 0}, \quad (39)$$

$$f_\pi^i = (\tilde{T}_{PA^i}^3 / q^i g_P)|_{q_0=0, \mathbf{q}\rightarrow 0}, \quad (40)$$

where the tilde indicates that the loop integral is with two factors of $\sqrt{\alpha}$ only, and because of the lack of $O(4)$ symme-

plotted in Fig. 5 (triangles) the same correlation functions at T_c if only the $U(1)$ symmetric molecule-induced interaction is included.

Because we obtain the correlation functions for Euclidean momenta by numerical procedure, we cannot analytically continue them and find the pole meson masses. However, the π mass is guaranteed by the Goldstone theorem to be 0. We can therefore derive the pion decay constants f_π and λ_π . The quark T matrix in the pseudoscalar, $I=1$ channel has the following form near the pion pole [see Fig. 2(d)]:

try, there are two f_π 's coupled to the time and the spatial components of the axial vector current. The results are shown in Fig. 6. g_A and the two f_π 's go to 0 at T_c as required by the restoration of the chiral symmetry. λ_π , however, remains finite. This means that the pion (and also his chiral partner σ), survive the phase transition. This conclusion is consistent with numerical evidence obtained from the calculation of the Euclidean correlation functions in the time direction [11], but there λ_π , although remaining finite, decreases towards T_c , while in our calculation λ_π slightly increases. This difference, as we have mentioned before, might be due to the nonzero quark current masses in [11].

Furthermore, in our approach we have found a signal of attractive interaction also in the vector (ρ) channel. It is seen as an additional maximum in the correlators, shown in Fig. 5(i), which is the same as the one, generated by the molecule-induced interaction (triangles). This signal was *not* observed in [10].¹²

VI. SUMMARY

In this paper we studied individual instanton-anti-instanton molecules, in much greater details than was done before. We determined classical bosonic interaction in the ratio ansatz and quark-induced interaction. Then we performed 11-dimensional integration over collective variables, 10 in the saddle-point approximation, and the last one explicitly.

The results obtained have been used in studies of molecule formation in the ensemble, at temperatures close to

¹⁰The issue of $U_A(1)$ restoration was debated in the literature for some time. One clearly cannot claim exact restoration, as is obvious from the fact that very small instantons violate it but do not care about the magnitude of T . However, for $N_f > 2$ massless flavors (which we do not discuss), the manifestations of the $U_A(1)$ violation are not visible in the η' channel and can only be found in states with more quarks.

¹¹This is an artifact of the ‘‘randomness’’ of the instanton liquid related to too strong fluctuations of the topological charge: it disappears in the interacting instanton liquid.

¹²One possible explanation is related to the different treatment of the nonzero mode part of the quark propagator. In [10] an additional repulsive interaction is included. The same authors did simulations with the free propagator, that we use, for the nonzero mode of the quark propagator and they noticed an attractive correlation function in the ρ channel. However, some other contributions are not included in both approaches (e.g., the confinement, which provides an attractive interaction). So the question of whether ρ ‘‘melts’’ below or at T_c remains open.

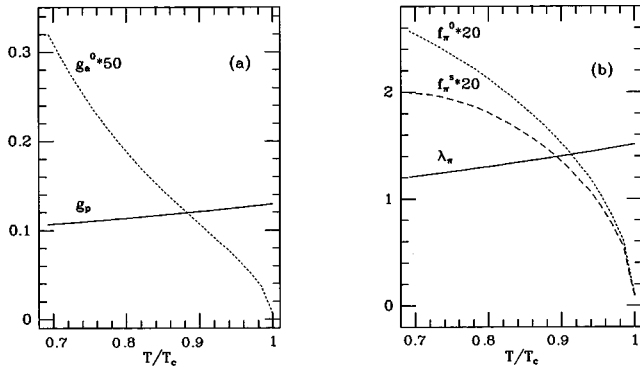


FIG. 6. The effective pion-quark couplings g_P and g_A (a) and the pion constants λ_π , f_π^0 , and f_π^i (b) as a function of the temperature. All dimensional quantities are in units of the inverse instanton radius $1/\rho = 580$ MeV.

chiral restoration point $T \approx T_c$. We have used a semianalytic two-component (or ‘‘cocktail’’) model, with contributions from uncorrelated instanton liquid and polarized $I\bar{I}$ molecules, and have confirmed that chiral restoration is driven by formation of the instanton–anti-instanton molecules.

Both random and molecular components have generated an effective four-fermion interaction. With standard mean field methods we have derived semianalytically the thermodynamics of the system. The basic conclusion is that there is

a rapid temperature dependence of the fraction of molecules f , see Fig. 3(a), which jumps from $f \sim 0.5$ at $T = 0.7T_c$ to 1 at T_c . The corresponding jump in energy density is strongly correlated with it [see Fig. 4(b)], confirming the idea suggested in [23] that formation of ‘‘molecules’’ is the major reason of rapid growth of the energy density around the phase transition point.

We have also calculated the mesonic correlation functions, using Bethe-Salpeter-type equation. We have found that the pion is decoupled from the axial current at T_c , as it should, but remains coupled to the pseudoscalar one even in pure molecular vacuum ($f = 1$). A strong signal has been found that, unlike the one reported numerically in [11], does not decrease with the temperature, indicating that the pion survives the phase transition as a bound state and that its radius does not swell at T_c . The σ meson follows the pattern of chiral symmetry restoration, joining the pion. The ‘‘repulsive’’ channels η , δ show an increase of the correlators, indicating strongly decreasing masses. Nevertheless, they do not exactly join the pion and the σ ones, so $U(1)_A$ symmetry remains noticeably broken.

ACKNOWLEDGMENTS

We would like to thank J. J. M. Verbaarschot for the many useful discussions. The reported work was partially supported by the U.S. DOE Grant No. DE-FG-88ER40388.

-
- [1] F. Karsch, in *Lattice 93*, Proceedings of the International Symposium, Dallas, Texas, edited by T. Draper *et al.* [Nucl. Phys. B (Proc. Suppl.) **34**, 63 (1994)].
- [2] C. DeTar, in *Lattice 94*, Proceedings of the International Symposium, Bielefeld, Germany, edited by F. Karsch *et al.* [Nucl. Phys. B (Proc. Suppl.) **42** (1995)]; in *Quark Gluon Plasma 2*, edited by R. Hwa (World Scientific, Singapore, 1995).
- [3] E. V. Shuryak, Nucl. Phys. **B203**, 93 (1982); **B203**, 116 (1982).
- [4] D. I. Diakonov and V. Yu. Petrov, Zh. Eksp. Teor. Fiz. **89**, 361 (1985) [Sov. Phys. JETP **62**, 204 (1985)]; Nucl. Phys. **B272**, 457 (1986).
- [5] D. I. Diakonov and V. Yu. Petrov, in *Hadron Matter Under Extreme Conditions*, Kiev, 1986 (unpublished), p. 192.
- [6] M. A. Nowak, J. J. M. Verbaarschot, and I. Zahed, Nucl. Phys. **B324**, 1 (1989).
- [7] E. Shuryak, Nucl. Phys. **B302**, 559 (1988); **B302**, 574 (1988); **B302**, 599 (1988); **B319**, 521 (1989); **B319**, 541 (1989).
- [8] E. V. Shuryak and J. J. M. Verbaarschot, Nucl. Phys. **B341**, 1 (1990).
- [9] E. V. Shuryak and J. J. M. Verbaarschot, Nucl. Phys. **B410**, 55 (1993); T. Schäfer, E. V. Shuryak, and J. J. M. Verbaarschot, *ibid.* **B412**, 143 (1994); T. Schäfer and E. V. Shuryak, Phys. Rev. D **50**, 478 (1994).
- [10] T. Schäfer and E. V. Shuryak, Phys. Rev. Lett. **75**, 1707 (1995).
- [11] T. Schäfer and E. V. Shuryak, Phys. Lett. B **356**, 147 (1995).
- [12] E. Shuryak, Rev. Mod. Phys. **65**, 1 (1993).
- [13] M. C. Chu, J. M. Grandy, S. Huang, and J. W. Negele, Phys. Rev. Lett. **70**, 225 (1993); M. C. Chu and S. Huang, Phys. Rev. D **45**, 2446 (1992).
- [14] M. C. Chu, J. M. Grandy, S. Huang, and J. W. Negele, Phys. Rev. D **49**, 6039 (1994).
- [15] C. Michael and P. S. Spencer, in *Lattice 94* [2], p. 261; Phys. Rev. D **50**, 7570 (1994).
- [16] S. Thurner, M. Feurstein, and H. Markum, Report No. hep-lat/9606011, 1996 (unpublished).
- [17] E. Shuryak, Phys. Lett. **79B**, 135 (1978).
- [18] R. D. Pisarski and L. G. Yaffe, Phys. Lett. **97B**, 110 (1980).
- [19] E. M. Ilgenfritz and E. Shuryak, Nucl. Phys. **B319**, 511 (1989).
- [20] E. Shuryak and M. Velkovsky, Phys. Rev. D **50**, 3323 (1994).
- [21] M. C. Chu and S. Schramm, Phys. Rev. D **51**, 4580 (1995).
- [22] E. M. Ilgenfritz and E. V. Shuryak, Phys. Lett. B **325**, 263 (1994).
- [23] T. Schäfer, E. V. Shuryak, and J. J. M. Verbaarschot, Phys. Rev. D **51**, 1267 (1995).
- [24] E. V. Shuryak and J. J. M. Verbaarschot, Nucl. Phys. **B364**, 255 (1991).
- [25] T. Schäfer and E. V. Shuryak, Phys. Rev. D **53**, 6522 (1996); **54**, 1099 (1996).
- [26] J. J. M. Verbaarschot, Nucl. Phys. **B362**, 33 (1991).
- [27] D. I. Diakonov and V. Yu. Petrov, Nucl. Phys. **B245**, 259 (1984).
- [28] C. Bernard, Phys. Rev. D **19**, 3013 (1979).
- [29] Edward Shuryak, Comments Nucl. Part. Phys. **21**, 235 (1994).
- [30] G. 't Hooft, Phys. Rev. D **14**, 3432 (1976).
- [31] M. A. Nowak, J. J. M. Verbaarschot, and I. Zahed, Nucl. Phys. **B325**, 581 (1989).

- [32] D. J. Gross, R. D. Pisarski, and L. G. Yaffe, *Rev. Mod. Phys.* **53**, 43 (1981).
- [33] S. Klimt, M. Lutz, U. Vogl, and W. Weise, *Nucl. Phys.* **A516**, 429 (1990).
- [34] U. Vogl and W. Weise, *Prog. Part. Nucl. Phys.* **27**, 195 (1991).
- [35] G. Boyd, S. Gupta, F. Karsch, and E. Laermann, *Z. Phys. C* **64**, 331 (1994).
- [36] T. D. Cohen, *Phys. Rev. D* **54**, 1867 (1996).
- [37] S. Lee and T. Hatsuda, *Phys. Rev. D* **54**, 1871 (1996).
- [38] N. Evans, S. D. H. Hsu, and M. Schwetz, *Phys. Lett. B* **375**, 262 (1996).